frontiers in Materials

ORIGINAL RESEARCH
published: 27 August 2019
doi: 10.3389/fmats.2019.00200

In-situ Interfacial Passivation for Stable Perovskite Solar Cells

Longfan Duan[1†], Liang Li[2†], Yizhou Zhao[1], Guangyue Cao[1], Xiuxiu Niu[1], Huanping Zhou[2], Yang Bai[1] and Qi Chen[1]*

[1] School of Materials Science and Engineering, Beijing Institute of Technology, Beijing, China, [2] College of Engineering, Peking University, Beijing, China

Unreacted lead iodide is commonly believed playing an important role in the performance of perovskite solar cells (PSCs). However, the excess lead iodide acts like a double-edged blade, which hampers the long-term stability of devices. Here, we used the ethanedithiol (EDT) as the solvent to process Spiro-OMeTAD (Spiro) layer. Due to the strong coordination between EDT and Pb (II), the unreacted PbI_2 at the perovskite films surface was effectively passivated, which suppressed the degradation of the perovskite layer without sacrificing the efficiency. Moreover, the hydrophobic EDT also enhanced the moisture stability of devices, thus prolonged the device lifetime. With EDT-Spiro layer, a stabilized power conversion efficiencies from 17.11% up to 19.23% was achieved in the corresponding device. More importantly, a significant enhancement of the long-term stability of PSCs was observed under the N_2 atmosphere without sealing for 30 days.

Keywords: dithiol, stability, interface, perovskite solar cell, efficiency

OPEN ACCESS

Edited by:
Xingang Ren,
Anhui University, China

Reviewed by:
Jianxin Tang,
Soochow University, China
Haifei Lu,
Wuhan University of Technology, China

****Correspondence:***
Qi Chen
qic@bit.edu.cn

[†]These authors have contributed equally to this work

Specialty section:
This article was submitted to Energy Materials, a section of the journal Frontiers in Materials

Received: *03 June 2019*
Accepted: *05 August 2019*
Published: *27 August 2019*

Citation:
Duan L, Li L, Zhao Y, Cao G, Niu X, Zhou H, Bai Y and Chen Q (2019) In-situ Interfacial Passivation for Stable Perovskite Solar Cells. Front. Mater. 6:200. doi: 10.3389/fmats.2019.00200

INTRODUCTION

Solar energy-to-electricity power conversion efficiency (PCE) of perovskite solar cells (PSCs) has rapidly improved from 3 to 24.2% in the past few years (Kojima et al., 2009; Yao et al., 2019). The reason for the excellent performance lies in the unique features of organometal halide perovskite materials APbX3 (A = methylammonium or formamidinium; X = Cl, Br, or I) such as high absorption coefficient, long charge carrier diffusion lengths, high carrier mobility, ambipolar charge transport properties, low exciton binding energy, and charge trap densities (Stranks et al., 2013; Xing et al., 2013; Saidaminov et al., 2015), and so on. Although the efficiency of PSCs have rapidly increased in recent years, however, there are still some major challenges need to be solved, especially the instability under moisture and continuous illumination, which hinders the pace for commercialization.

Several methods had been proposed to enhance the stability of perovskite. Seok and co-workers employed the mixed-halide perovskites $CH_3NH_3Pb(I_{1-x}Br_x)_3$ as the absorbed layer in PSCs to prolong the lifetime of devices (Jeon et al., 2014). Snaith et al. tested the stability of $NH_2 = CHNH_2PbI_3$ and $CH_3NH_3PbI_3$ films at 150°C in air and observed the latter was fade quickly than the former (Cheacharoen et al., 2018). McGehee et al. showed the mixed halide PSCs could withstand a 1,000 h damp heat test under 85°C and 85% relative humidity (Eperon et al., 2014).

Moreover, in the components of PSCs, hole-transporting material (HTM) not only plays an important role in charge transfer, but also can prevent the perovskite film from directly contact with moisture and oxygen from the air. To date, Spiro-OMeTAD(Spiro) has been proved to be an excellent HTM for highly efficient PSCs due to its desirable properties, such as low glass transition temperature, high solubility, suitable work function as well as good film quality (Kim et al., 2012). In addition, Qi et al. observed that pinholes existed at the surface of Spiro film, and they demonstrated that the using of chlorobenzene was the main reason for the pinhole formation. By changing the solvent from chlorobenzene to chloroform, they successfully deposited a pinhole-free Spiro film (Ono et al., 2014; Hawash et al., 2015). Meng et al. used ethyl acetate as the solvent for perovskite and Spiro layers, which enabled a synergic interface (perovskite/Spiro) optimization and greatly improved efficiency and stability compared with CB-Spiro devices (Bu et al., 2017). Sargent et al. used thiol-terminated ligands in colloidal quantum dot photovoltaic devices to passivate recombination centers which enhanced 10-fold of the PCE (Barkhouse et al., 2008; Klem et al., 2008). Thiols are known to interact readily with metal nanoparticles and are expected to coordinate with the PbI_2 on the surface of perovskite films to enhance the stability of perovskite film. Moreover, EDT is known to hydrophobic, so it could protect perovskite layers from water thus help to improve the device long-term stability.

In this work, we demonstrate a convenient methodology for preparing high quality Spiro films by changing the solvent from the commonly used CB to EDT to cooperate with the unreacted PbI_2 at the film surface. Compared with the CB-Spiro devices, the EDT-Spiro devices show an excellent long-term stability in the N_2 atmosphere without sealing. At the same time, EDT-Spiro devices employed a smaller defects level and enhanced charge carrier transfer behavior. As a result, PSCs with EDT-Spiro exhibit an average PCE of 17.45%, representing an increase of 24% over the 14.00% average PCE of the CB-Spiro devices and maintaining over 75% of its original efficiency after stored under N_2 environment for 30 days. Therefore, our results reveal that EDT is an excellent solution for Spiro to highly efficient and stable PSCs.

RESULTS AND DISCUSSION

The top-view scanning electron microscope (SEM) image of perovskite film is shown in **Figure 1A**. It can be seen from the SEM image that a small amount of excess PbI_2 is existed at the surface of perovskite film. The unreacted PbI_2 has been proved having positive effects on the device performance but damaging the device stability at the same time (Liu et al., 2016). Therefore, it's crucial to reduce the PbI_2 on the surface to minimize its influence on the stability. EDT are known to interact readily with the heavily metal such as Pb atoms as shown in **Figure 1B**, which is expected to coordinate with the PbI_2 at the surface of perovskite films (Mah and Jalilehvand, 2012). **Figure 1C** presents the XRD patterns of perovskite films processed with EDT and CB. Compared with CB processed film, the peak of PbI_2

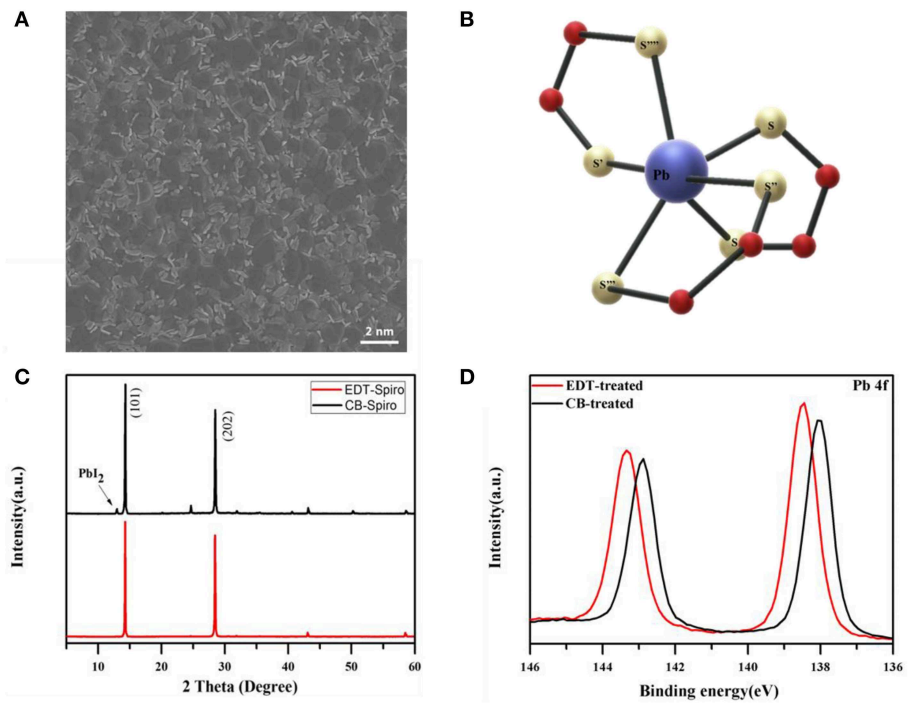

FIGURE 1 | (A) SEM images of the top view of perovskite films. **(B)** The model for Pb(II) cooperate with EDT. **(C)** XRD patterns of perovskite films processed with EDT and CB. **(D)** XPS spectra of Pb 4f with the CB and EDT solvents processed perovskite films.

disappeared after the film processed with EDT, which indicated the coordination between EDT and PbI_2 (Liu et al., 2018). To further understand the interaction between PbI_2 and EDT, X-ray photoelectron spectroscopy (XPS) was employed. As shown in **Figure 1D**, for the CB processed film, two main peaks located at 138.0 and 142.8 eV were observed, which were assigned to the Pb 4f 7/2 and Pb 4f 5/2, respectively. However, with EDT processed perovskite film, the binding energy of Pb 4f was increased by 0.6, which indicated that the Pb coordinated with a atom of higher electron affinity. And the peaks located at 138.6 and 143.4 eV confirmed that the EDT molecule anchors to the perovskite surface via Pb–S coordination (Odio et al., 2016).

The SEM images of the Spiro film on perovskite are presented in **Figures 2A–D**, which show the quality difference of Spiro films prepared by using CB and EDT solvents. The CB-Spiro film have poor dispersion and attempt to aggregate after spin-coating process (show in **Figure 2A**). It could be ascribed to the residue of the CB solvent. The higher boiling point of CB (132°C for CB and

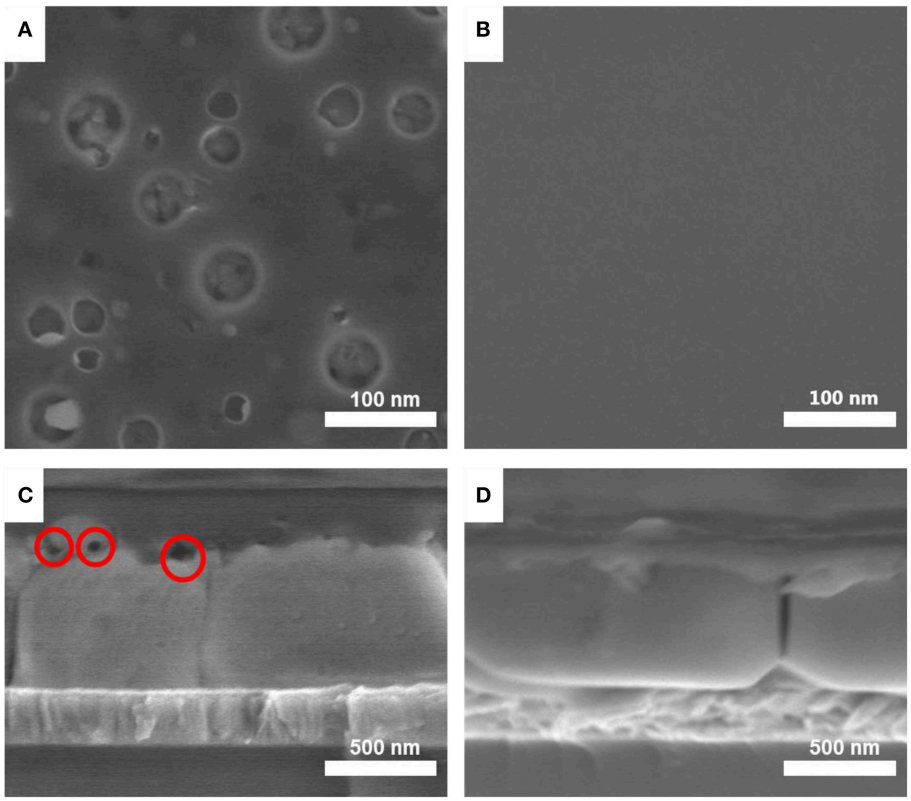

FIGURE 2 | The top view SEM images of **(A)** CB-Spiro and **(B)** EDT-Spiro films as well as the cross-sectional SEM images of **(C)** the CB-Spiro and **(D)** EDT-Spiro films deposited on the perovskite films.

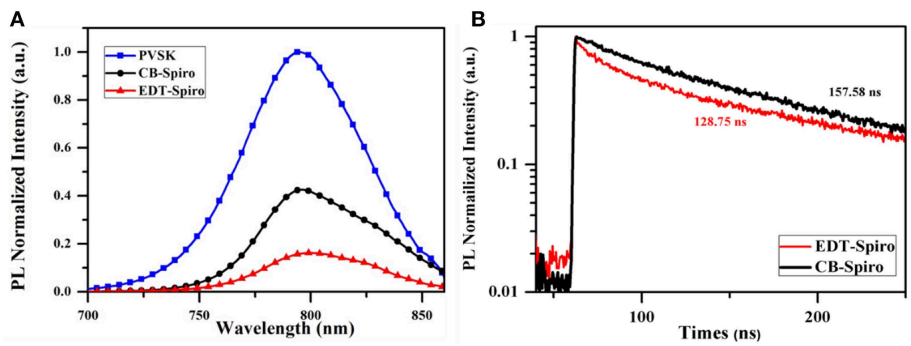

FIGURE 3 | (A) Photoluminescence spectrum of glass/FTO/SnO_2/PVSK/CB-Spiro and glass/FTO/SnO_2/PVSK/ EDT-Spiro, respectively. **(B)** Time-resolved photoluminescence spectra (at 795 nm) of the CB-Spiro and EDT-Spiro films, respectively.

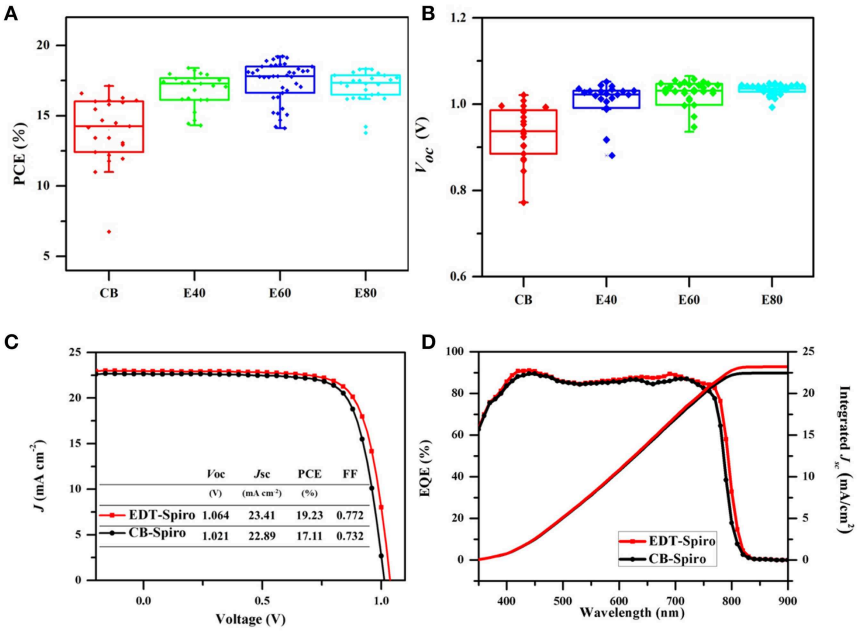

FIGURE 4 | The **(A)** PCE and **(B)** V_{OC} of the different density EDT-Spiro solvents processed perovskite solar cells. **(C)** *J-V* curves of the CB and EDT devices under forward scan. **(D)** The external quantum efficiency (EQE) of the best CB and EDT devices.

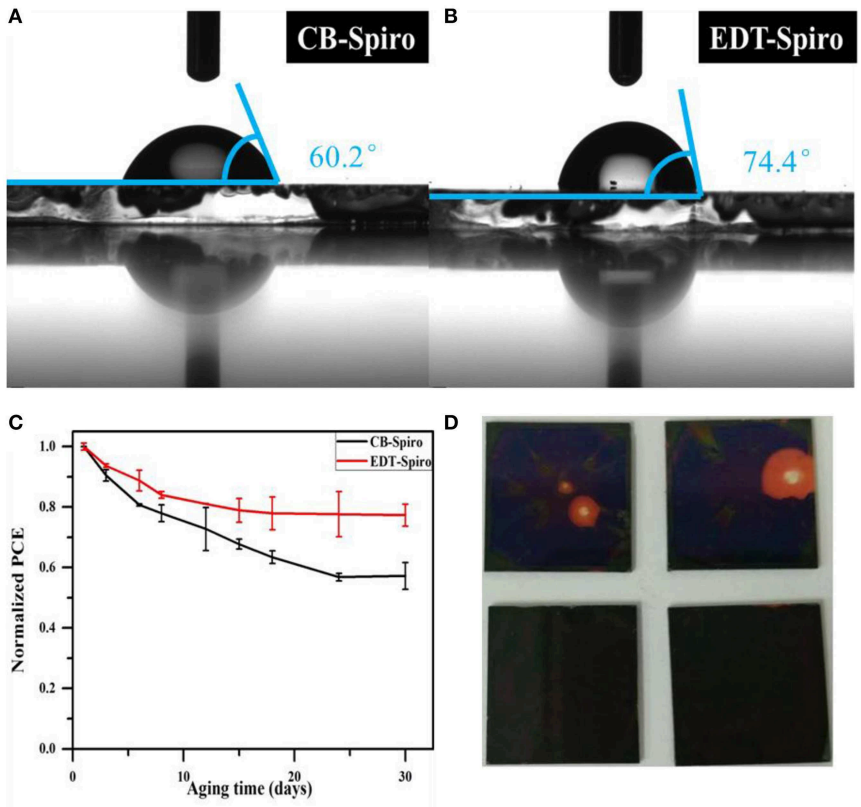

FIGURE 5 | (A) The water contact angles of CB-Spiro films and **(B)** EDT-Spiro films. **(C)** Stability test of the best CB and EDT devices under N_2 atmosphere without sealing. **(D)** Photos of CB-Spiro (the above one) and the EDT-Spiro (the below one) films upon in the O_2 atmosphere for 2 days.

36.2°C for EDT) leads to much slower drying during the spin-coating. Besides that, there are also some voids at the interfaces of Spiro/perovskite for the CB processed film as shown in the cross-sectional SEM images in **Figure 2C**. However, the Spiro and perovskite film contact tightly in the EDT processed film. The existence of the interface voids would affect the charge extraction at the Spiro/perovskite interfaces. Thus, the enhancing of the film quality with reduction of voids could significantly improve the device's performance.

Interfaces in the PSCs play a crucial role to carries diffusion and recombination, thus affect the photovoltaic performance and stability (Zhou et al., 2014; Shi et al., 2015; Fan et al., 2016). To further understand the charge extraction behavior at the interface of Spiro/perovskite layer, the steady-state and time-resolved transient- photoluminescence spectrum of samples with corresponding structures. As shown in the **Figure 3A**, the perovskite film exhibits a strong emission peak at 795 nm due to the radiative recombination. For the perovskite film covered with CB processed Spiro layer, the emission is apparently suppressed due to the charge extraction from perovskite to Spiro. More importantly, the sample with EDT processed Spiro film shows the strongest quenching of PL intensity. The above results indicates that the interface of perovskite/EDT-Spiro employs a faster charge extraction rate than that of perovskite/CB-Spiro. This results are also proved by the time-resolved PL spectra as shown in **Figure 3B**. The fitted photoluminescence decay times of the CB-Spiro and EDT-Spiro are 157.58 and 128.75 ns, which indicated that more efficient carrier extraction. The faster charge transfer of EDT-Spiro layer benefits the short-circuit current (J_{sc}) of the PSCs (as shown in **Supplementary Figure 1**).

CB-Spiro and EDT-Spiro solution with different concentrations of 40, 60, 80 mg/ml (named E40, E60, and E80) was deposited on the perovskite film to optimize devices performance. **Figure 4A** shows that the PCE was increased with the increased of concentration of EDT-Spiro at the range of 40–60 mg/ml, which is attributed to the increase of V_{oc} (**Figure 4**B), indicating that EDT improved the electron transfer between the perovskite/Spiro interface with reduced charge recombination (Zhao and Zhu, 2013; Zarazua et al., 2016; Yadav et al., 2017). Further increase the concentration to 80 mg/ml EDT-Spiro resulted in a decrease in J_{sc} and fill factor (FF), which is due to the increased series resistance with the thicker Spiro film (Pockett et al., 2015). The best performance was obtained from EDT-Spiro of concentration of 60 mg/ml with V_{oc}, J_{sc}, FF, and PCE of 1.064 V, 23.41 mA cm^{-2}, 77.18 and 19.23%, respectively. The external quantum efficiency (EQE) spectra (**Figure 4D**) shows that the devices effectively harvest light across the entire visible spectral region. The integrated current density of 23.19 mA cm^{-2} calculated from the EQE data is in good agreement with the J_{sc} value of 23.41 mA cm^{-2} measured from the best performing device. For comparison, the J-V performance of the best EDT-Spiro based and the CB-Spiro device are shown in **Figure 4C**.

In addition, EDT is a hydrophobic material and is expected to protect perovskite layers from moisture to improve the long-term stability of device. As can be seen from **Figures 5A,B**, for the EDT-Spiro film, the water contact angle increased to 74.4° (**Figure 5B**), which is much bigger than that of CB-treat films (**Figure 5A**), so that the EDT-Spiro can efficiently prevent the water penetration into the perovskite layer. **Figure 5C** shows the PCE track of PSCs devices stored under N_2 atmosphere without sealing for 30 days. Compared with the CB-Spiro devices, the EDT-Spiro devices showed better stability which remains 75% of its initial efficiency after 30 days. However, the efficiency of the CB-Spiro device had decreased by over 40%. The detailed data of V_{oc}, J_{sc}, and FF vs. the aging time (**Supplementary Figure 2**) reveal that the efficiency decay was mainly originated from the decreasing of fill factor. The photos of perovskite films with CB-Spiro and EDT-Spiro are shown in **Figure 5D** to demonstrate the change of film color after long time aging. It can be seen from this photos that the one with CB-Spiro film shows obvious changes, which indicates the decomposition of perovskite film. At the same time, the one with EDT-Spiro shows negligible change on the film, indicating the better stability which may contributed by the better water-proof ability of the EDT-Spiro as well as the elimination of surface unreacted PbI_2.

CONCLUSION

In summary, we employed EDT as the solvent for Spiro deposition and investigated the performance and stability of PSCs. Compared with CB processed Spiro, the EDT processed Spiro presented an improved stabilized power conversion efficiencies from 17.11% up to 19.23% with average efficiencies increased from 14.00 to 17.45%. Moreover, a significant enhancement of the long-term stability of PSCs was obtained in the N_2 atmosphere without sealing. The enhanced stability of the EDT device is mainly attributed to the EDT-Spiro could effectively passivated with the excess PbI_2 on the perovskite films and suppress the degradation of the perovskite layer which as well as the larger water contact angle of EDT processed Spiro. The XRD and XPS spectra also revealed the strong interaction between EDT and PbI_2 on the perovskite films. The photoluminescence result clearly illustrates that the interface of perovskite/EDT-Spiro employed faster charge extraction rate than that of perovskite/CB-Spiro. Thus, the use of EDT to dissolve the Spiro obviously reduces the defects and carrier traps at the perovskite/EDT-Spiro interface. Hopefully the current research project will lead to a new processing approach for fabrication of high efficiency and long-term stability PSC based on novel solvents for HTMs, which facilitates the commercialization of perovskite electronics.

DATA AVAILABILITY

All datasets generated for this study are included in the manuscript/**Supplementary Files**.

AUTHOR CONTRIBUTIONS

LL, YB, and QC conceived the original idea and suggested on the experiment framework. LD and LL co-carried out the experiment. LD wrote the manuscript with support from LL

and YB. YZ and XN drew the scheme. All authors provided critical feedback and helped shape the research, analysis, and manuscript.

FUNDING

This work was supported by National Key Research and Development Program of China (Grant No. 2016YFB0700700), National Natural Science Foundation of China (51673025), Beijing Municipal Science and Technology Project No. Z181100005118002, and the Young Talent Thousand Program.

SUPPLEMENTARY MATERIAL

The Supplementary Material for this article can be found online at: https://www.frontiersin.org/articles/10.3389/fmats.2019.00200/full#supplementary-material

REFERENCES

Barkhouse, D. A., Pattantyus-Abraham, A. G., Levina, L., and Sargent, E. H. (2008). Thiols passivate recombination centers in colloidal quantum dots leading to enhanced photovoltaic device efficiency. *ACS Nano* 2, 2356–2362. doi: 10.1021/nn800471c

Bu, T., Wu, L., Liu, X., Yang, X., Zhou, P., Yu, X., et al. (2017). Synergic interface optimization with green solvent engineering in mixed perovskite solar cells. *Adv. Energy Mater.* 7:1700576. doi: 10.1002/aenm.201700576

Cheacharoen, R., Boyd, C. C., Burkhard, G. F., Leijtens, T., Raiford, J. A., Bush, K. A., et al. (2018). Encapsulating perovskite solar cells to withstand damp heat and thermal cycling. *Sustain. Energy Fuels* 2, 2398–2406. doi: 10.1039/C8SE00250A

Eperon, G. E., Stranks, S. D., Menelaou, C., Johnston, M., Herz, L. M., and Snaith, H. J. (2014). Formamidinium lead trihalide: a broadly tunable perovskite for efficient planar heterojunction solar cells. *Energy Environ. Sci.* 7:982. doi: 10.1039/c3ee43822h

Fan, R., Huang, Y., Wang, L., Li, L., Zheng, G., and Zhou, H. (2016). The progress of interface design in perovskite-based solar cells. *Adv. Energy Mater.* 6:1600460. doi: 10.1002/aenm.201600460

Hawash, Z., Ono, L. K., Raga, S. R., Lee, M., and Qi, Y. (2015). Air-exposure induced dopant redistribution and energy level shifts in Spin-Coated Spiro-MeOTAD films. *Chem. Mater.* 27, 562–569. doi: 10.1021/cm504022q

Jeon, N. J., Noh, J. H., Kim, Y. C., Yang, W. S., Ryu, S., and Seok, S. I. (2014). Solvent engineering for high-performance inorganic–organic hybrid perovskite solar cells. *Nat. Mater.* 13:897. doi: 10.1038/nmat4014

Kim, H. S., Lee, C. R., Im, J. H., Lee, K. B., Moehl, T., Marchioro, A., et al. (2012). Lead iodide perovskite sensitized all-solid-state submicron thin film mesoscopic solar cell with efficiency exceeding 9%. *Sci. Rep.* 2:591. doi: 10.1038/srep00591

Klem, E. J. D., Shukla, H., Hinds, S., MacNeil, D. D., Levina, L., and Sargent, E. H. (2008). Impact of dithiol treatment and air annealing on the conductivity, mobility, and hole density in PbS colloidal quantum dot solids. *Appl. Phys. Lett.* 92:212105. doi: 10.1063/1.2917800

Kojima, A., Teshima, K., Shirai, Y., and Miyasaka, T. (2009). Organometal halide perovskites as visible-light sensitizers for photovoltaic cells. *J. Am. Chem. Soc.* 131, 6050–6051. doi: 10.1021/ja809598r

Liu, F., Dong, Q., Wong, M. K., Djurišić, A. B., Ng, A., Ren, Z., et al. (2016). Is excess PbI, beneficial for perovskite solar cell performance? *Adv. Energy Mater.* 6:1502206. doi: 10.1002/aenm.201502206

Liu, L., Huang, S., Lu, Y., Liu, P., Zhao, Y., Shi, C., et al. (2018). Grain-boundary "patches" by *in situ* conversion to enhance perovskite solar cells stability. *Adv. Mater.* 30:1800544. doi: 10.1002/adma.201800544

Mah, V., and Jalilehvand, F. (2012). Lead(II) complex formation with glutathione. *Inorg. Chem.* 51, 6285–6298. doi: 10.1021/ic300496t

Odio, O. F., Lartundo-Rojas, L., Palacios, E. G., Martinez, R., and Reguera, E. (2016). Synthesis of a novel poly-thiolated magnetic nano-platform for heavy metal adsorption. Role of thiol and carboxyl functions. *Appl. Surf. Sci.* 386, 160–177. doi: 10.1016/j.apsusc.2016.05.176

Ono, L. K., Schulz, P., Endres, J. J., Nikiforov, G. O., Kato, Y., Kahn, A., et al. (2014). Air-exposure-induced gas-molecule incorporation into Spiro-MeOTAD films. *J. Phys. Chem. Lett.* 5, 1374–1379. doi: 10.1021/jz500414m

Pockett, A., Eperon, G. E., Peltola, T., Snaith, H. J., Walker, A., Peter, L. M., et al. (2015). Characterization of planar lead halide perovskite solar cells by impedance spectroscopy, open-circuit photovoltage decay, and intensity-modulated photovoltage/photocurrent spectroscopy. *J. Phys. Chem. C* 119, 3456–3465. doi: 10.1021/jp510837q

Saidaminov, M. I., Abdelhady, A. L., Murali, B., Alarousu, E., Burlakov, V. M., Peng, W., et al. (2015). High-quality bulk hybrid perovskite single crystals within minutes by inverse temperature crystallization. *Nat. Commun.* 6:7586. doi: 10.1038/ncomms8586

Shi, J., Xu, X., Li, D., and Meng, Q. (2015). Interfaces in perovskite solar cells. *Small* 11, 2472–2486. doi: 10.1002/smll.201403534

Stranks, S. D., Eperon, G. E., Grancini, G., Menelaou, C., Alcocer, M. J., Leijtens, T., et al. (2013). Electron-hole diffusion lengths exceeding 1 micrometer in an organometal trihalide perovskite absorber. *Science* 342, 341–344. doi: 10.1126/science.1243982

Xing, G., Mathews, N., Sun, S., Lim, S. S., Lam, Y. M., Grätzel, M., et al. (2013). Long-range balanced electron- and hole-transport lengths in organic-inorganic $CH_3NH_3PbI_3$. *Science* 342, 344–347. doi: 10.1126/science.1243167

Yadav, P., Dar, M. I., Arora, N., Alharbi, E. A., Giordano, F., Zakeeruddin, S. M., et al. (2017). The role of rubidium in multiple-cation-based high-efficiency perovskite solar cells. *Adv. Mater.* 29:1701077. doi: 10.1002/adma.201701077

Yao, H., Cui, Y., Qian, D., Ponseca, C. S., Honarfar, A., Xu, Y., et al. (2019). 14.7% efficiency organic photovoltaic cells enabled by active materials with a large electrostatic potential difference. *J. Am. Chem. Soc.* 141:7743 doi: 10.1021/jacs.8b12937

Zarazua, I., Han, G., Boix, P. P., Mhaisalkar, S., Fabregat-Santiago, F., Mora-Seró, I., et al. (2016). Surface recombination and collection efficiency in perovskite solar cells from impedance analysis. *J. Phys. Chem. Lett.* 7, 5105–5113. doi: 10.1021/acs.jpclett.6b02193

Zhao, Y., and Zhu, K. (2013). Charge transport and recombination in perovskite $(CH_3NH_3)PbI_3$ sensitized TiO_2 solar cells. *J. Phys. Chem. Lett.* 4, 2880–2884. doi: 10.1021/jz401527q

Zhou, H., Chen, Q., Li, G., Luo, S., Song, T. B., Duan, H. S., et al. (2014). Photovoltaics. Interface engineering of highly efficient perovskite solar cells. *Science* 345, 542–546. doi: 10.1126/science.1254050

Conflict of Interest Statement: The authors declare that the research was conducted in the absence of any commercial or financial relationships that could be construed as a potential conflict of interest.